Available online at www.sciencedirect.com
ScienceDirect
International Journal of Plasticity 23 (2007) 1874–1900
INTERNATIONAL JOURNAL OF Plasticity
www.elsevier.com/locate/ijplas

A plasticity and anisotropic damage model for plain concrete

Umit Cicekli, George Z. Voyiadjis *, Rashid K. Abu Al-Rub

Department of Civil and Environmental Engineering, Louisiana State University, CEBA 3508-B, Baton Rouge, LA 70803, USA

Received 23 April 2006; received in final revised form 29 October 2006
Available online 15 March 2007

Abstract

A plastic-damage constitutive model for plain concrete is developed in this work. Anisotropic damage with a plasticity yield criterion and a damage criterion are introduced to be able to adequately describe the plastic and damage behavior of concrete. Moreover, in order to account for different effects under tensile and compressive loadings, two damage criteria are used: one for compression and a second for tension such that the total stress is decomposed into tensile and compressive components. Stiffness recovery caused by crack opening/closing is also incorporated. The strain equivalence hypothesis is used in deriving the constitutive equations such that the strains in the effective (undamaged) and damaged configurations are set equal. This leads to a decoupled algorithm for the effective stress computation and the damage evolution. It is also shown that the proposed constitutive relations comply with the laws of thermodynamics. A detailed numerical algorithm is coded using the user subroutine UMAT and then implemented in the advanced finite element program ABAQUS. The numerical simulations are shown for uniaxial and biaxial tension and compression. The results show very good correlation with the experimental data.

Keywords: Damage mechanics; Isotropic hardening; Anisotropic damage

* Corresponding author. Tel.: +1 225 578 8668; fax: +1 225 578 9176.
E-mail addresses: voyiadjis@eng.lsu.edu (G.Z. Voyiadjis), rabual1@lsu.edu (R.K. Abu Al-Rub).

0749-6419/$ - see front matter © 2007 Elsevier Ltd. All rights reserved.
doi:10.1016/j.ijplas.2007.03.006

1. Introduction

Concrete is a widely used material in numerous civil engineering structures. Due to its ability to be cast on site it allows to be used in different shapes in structures: arc, ellipsoid, etc. This increases the demand for use of concrete in structures. Therefore, it is crucial to understand the mechanical behavior of concrete under different loadings such as compression and tension, for uniaxial, biaxial, and triaxial loadings. Moreover, challenges in designing complex concrete structures have prompted the structural engineer to acquire a sound understanding of the mechanical behavior of concrete. One of the most important characteristics of concrete is its low tensile strength, particularly at low-confining pressures, which results in tensile cracking at a very low stress compared with compressive stresses. The tensile cracking reduces the stiffness of concrete structural components. Therefore, the use of continuum damage mechanics is necessary to accurately model the degradation in the mechanical properties of concrete. However, the concrete material undergoes also some irreversible (plastic) deformations during unloading such that the continuum damage theories cannot be used alone, particularly at high-confining pressures. Therefore, the nonlinear material behavior of concrete can be attributed to two distinct material mechanical processes: damage (micro-cracks, micro-cavities, nucleation and coalescence, decohesions, grain boundary cracks, and cleavage in regions of high stress concentration) and plasticity, which its mechanism in concrete is not completely understood up-to-date. These two degradation phenomena may be described best by theories of continuum damage mechanics and plasticity. Therefore, a model that accounts for both plasticity and damage is necessary. In this work, a coupled plastic-damage model is thus formulated.

Plasticity theories have been used successfully in modeling the behavior of metals where the dominant mode of internal rearrangement is the slip process. Although the mathematical theory of plasticity is thoroughly established, its potential usefulness for representing a wide variety of material behavior has not been yet fully explored. There are many researchers who have used plasticity alone to characterize the concrete behavior (e.g. Chen and Chen, 1975; William and Warnke, 1975; Bazant, 1978; Dragon and Mroz, 1979; Schreyer, 1983; Chen and Buyukozturk, 1985; Onate et al., 1988; Voyiadjis and Abu-Lebdeh, 1994; Karabinis and Kiousis, 1994; Este and Willam, 1994; Menetrey and Willam, 1995; Grassl et al., 2002). The main characteristic of these models is a plasticity yield surface that includes pressure sensitivity, path sensitivity, non-associative flow rule, and work or strain hardening. However, these works failed to address the degradation of the material stiffness due to micro-cracking. On the other hand, others have used the continuum damage theory alone to model the material nonlinear behavior such that the mechanical effect of the progressive micro-cracking and strain softening are represented by a set of internal state variables which act on the elastic behavior (i.e. decrease of the stiffness) at the macroscopic level (e.g. Loland, 1980; Ortiz and Popov, 1982; Krajcinovic, 1983, 1985; Resende and Martin, 1984; Simo and Ju, 1987a,b; Mazars and Pijaudier-Cabot, 1989; Lubarda et al., 1994). However, there are several facets of concrete behavior (e.g. irreversible deformations, inelastic volumetric expansion in compression, and crack opening/closure effects) that cannot be represented by this method, just as plasticity, by itself, is insufficient. Since both micro-cracking and irreversible deformations are contributing to the nonlinear response of concrete, a constitutive model should address equally the two physically distinct modes of irreversible changes and should satisfy the basic postulates of thermodynamics.

Combinations of plasticity and damage are usually based on isotropic hardening combined with either isotropic (scalar) or anisotropic (tensor) damage. Isotropic damage is widely used due to its simplicity such that different types of combinations with plasticity models have been proposed in the literature. One type of combination relies on stress-based plasticity formulated in the effective (undamaged) space (e.g. Yazdani and Schreyer, 1990; Lee and Fenves, 1998; Gatuingt and Pijaudier-Cabot, 2002; Jason et al., 2004; Wu et al., 2006), where the effective stress is defined as the average micro-scale stress acting on the undamaged material between micro-defects. Another type is based on stress-based plasticity in the nominal (damaged) stress space (e.g. Bazant and Kim, 1979; Ortiz, 1985; Lubliner et al., 1989; Imran and Pantazopoulu, 2001; Ananiev and Ozbolt, 2004; Kratzig and Polling, 2004; Menzel et al., 2005; Brünig and Ricci, 2005), where the nominal stress is defined as the macro-scale stress acting on both damaged and undamaged material. However, it is shown by Abu Al-Rub and Voyiadjis (2004) and Voyiadjis et al. (2003, 2004) that coupled plastic-damage models formulated in the effective space are numerically more stable and attractive. On the other hand, for better characterization of the concrete damage behavior, anisotropic damage effects, i.e. different micro-cracking in different directions, should be characterized. However, anisotropic damage in concrete is complex and a combination with plasticity and the application to structural analysis is straightforward (e.g. Yazdani and Schreyer, 1990; Abu-Lebdeh and Voyiadjis, 1993; Voyiadjis and Kattan, 1999; Carol et al., 2001; Hansen et al., 2001), and, therefore, it has been avoided by many authors.

Consequently, with inspiration from all the previous works, a coupled anisotropic damage and plasticity constitutive model that can be used to predict the concrete distinct behavior in tension and compression is formulated here within the basic principles of thermodynamics. The proposed model includes important aspects of the concrete nonlinear behavior. The model considers different responses of concrete under tension and compression, the effect of stiffness degradation, and the stiffness recovery due to crack closure during cyclic loading. The yield criterion that has been proposed by Lubliner et al. (1989) and later modified by Lee and Fenves (1998) is adopted. Pertinent computational aspects concerning the algorithmic aspects and numerical implementation of the proposed constitutive model in the well-known finite element code ABAQUS (2003) are presented. Some numerical applications of the model to experimental tests of concrete specimens under different uniaxial and biaxial tension and compression loadings are provided to validate and demonstrate the capability of the proposed model.

2. Modeling anisotropic damage in concrete

In the current literature, damage in materials can be represented in many forms such as specific void and crack surfaces, specific crack and void volumes, the spacing between cracks or voids, scalar representation of damage, and general tensorial representation of damage. Generally, the physical interpretation of the damage variable is introduced as the specific damaged surface area (Kachonov, 1958), where two cases are considered: isotropic (scalar) damage and anisotropic (tensor) damage density of micro-cracks and micro-voids. However, for accurate interpretation of damage in concrete, one should consider the anisotropic damage case. This is attributed to the evolution of micro-cracks in concrete whereas damage in metals can be satisfactorily represented by a scalar damage variable (isotropic damage) for evolution of voids. Therefore, for more reliable representation of concrete damage anisotropic damage is considered in this study.

The effective (undamaged) configuration is used in this study in formulating the damage constitutive equations. That is, the damaged material is modeled using the constitutive laws of the effective undamaged material in which the Cauchy stress tensor, σ_{ij}, can be replaced by the effective stress tensor, $\bar{\sigma}_{ij}$ (Cordebois and Sidoroff, 1979; Murakami and Ohno, 1981; Voyiadjis and Kattan, 1999):

$$\bar{\sigma}_{ij} = M_{ijkl}\sigma_{kl} \tag{1}$$

where M_{ijkl} is the fourth-order damage effect tensor that is used to make the stress tensor symmetrical. There are different definitions for the tensor M_{ijkl} that could be used to symmetrize σ_{ij} (see Voyiadjis and Park, 1997; Voyiadjis and Kattan, 1999). In this work the definition that is presented by Abu Al-Rub and Voyiadjis (2003) is adopted:

$$M_{ijkl} = 2[(\delta_{ij} - \varphi_{ij})\delta_{kl} + \delta_{ij}(\delta_{kl} - \varphi_{kl})]^{-1} \tag{2}$$

where δ_{ij} is the Kronecker delta and φ_{ij} is the second-order damage tensor whose evolution will be defined later and it takes into consideration different evolution of damage in different directions. In the subsequence of this paper, the superimposed dash designates a variable in the undamaged configuration.

The transformation from the effective (undamaged) configuration to the damaged one can be done by utilizing either the strain equivalence or strain energy equivalence hypotheses (see Voyiadjis and Kattan, 1999). However, in this work the strain equivalence hypothesis is adopted for simplicity, which basically states that the strains in the damaged configuration and the strains in the undamaged (effective) configuration are equal. Therefore, the total strain tensor ε_{ij} is set equal to the corresponding effective tensor $\bar{\varepsilon}_{ij}$ (i.e. $\varepsilon_{ij} = \bar{\varepsilon}_{ij}$), which can be decomposed into an elastic strain ε^{e}_{ij} $(=\bar{\varepsilon}^{e}_{ij})$ and a plastic strain $\varepsilon^{p}_{ij}(=\bar{\varepsilon}^{p}_{ij})$ such that:

$$\varepsilon_{ij} = \varepsilon^{e}_{ij} + \varepsilon^{p}_{ij} = \bar{\varepsilon}^{e}_{ij} + \bar{\varepsilon}^{p}_{ij} = \bar{\varepsilon}_{ij} \tag{3}$$

It is noteworthy that the physical nature of plastic (irreversible) deformations in concrete is not well-founded until now. Whereas the physical nature of plastic strain in metals is well-understood and can be attributed to the generation and motion of dislocations along slip planes. Therefore, in metals any additional permanent strains due to micro-cracking and void growth can be classified as a damage strain. These damage strains are shown by Abu Al-Rub and Voyiadjis (2003) and Voyiadjis et al. (2003, 2004) to be minimal in metals and can be simply neglected. Therefore, the plastic strain in Eq. (3) incorporates all types of irreversible deformations whether they are due to tensile micro-cracking, breaking of internal bonds during shear loading, and/or compressive consolidation during the collapse of the micro-porous structure of the cement matrix. In the current work, it is assumed that plasticity is due to damage evolution such that damage occurs before any plastic deformations. However, this assumption needs to be validated by conducting microscopic experimental characterization of concrete damage.

Using the generalized Hook's law, the effective stress is given as follows:

$$\bar{\sigma}_{ij} = \overline{E}_{ijkl}\varepsilon^{e}_{kl} \tag{4}$$

where $\overline{E}_{ijkl}$ is the fourth-order undamaged elastic stiffness tensor. For isotropic linear-elastic materials, $\overline{E}_{ijkl}$ is given by

$$\overline{E}_{ijkl} = 2\overline{G}I^{d}_{ijkl} + \overline{K}I_{ijkl} \tag{5}$$

where $I^d_{ijkl} = I_{ijkl} - \frac{1}{3}\delta_{ij}\delta_{kl}$ is the deviatoric part of the fourth-order identity tensor $I_{ijkl} = \frac{1}{2}(\delta_{ik}\delta_{jl} + \delta_{il}\delta_{jk})$, and $\overline{G} = \overline{E}/2(1+\nu)$ and $\overline{K} = \overline{E}/3(1-2\nu)$ are the effective shear and bulk moduli, respectively, with $\overline{E}$ being the Young's modulus and ν is the Poisson's ratio which are obtained from the stress–strain diagram in the effective configuration.

Similarly, in the damaged configuration the stress–strain relationship in Eq. (4) can be expressed by:

$$\sigma_{ij} = E_{ijkl}\varepsilon^{\mathrm{e}}_{kl} \tag{6}$$

such that one can express the elastic strain from Eqs. (4) and (5) by the following relation:

$$\varepsilon^{\mathrm{e}}_{ij} = E^{-1}_{ijkl}\sigma_{kl} = \overline{E}^{-1}_{ijkl}\bar{\sigma}_{kl} \tag{7}$$

where E^{-1}_{ijkl} is the inverse (or compliance tensor) of the fourth-order damaged elastic tensor E_{ijkl}, which are a function of the damage variable φ_{ij}.

By substituting Eq. (1) into Eq. (7), one can express the damaged elasticity tensor E_{ijkl} in terms of the corresponding undamaged elasticity tensor $\overline{E}_{ijkl}$ by the following relation:

$$E_{ijkl} = M^{-1}_{ijmn}\overline{E}_{mnkl} \tag{8}$$

Moreover, combining Eqs. (3) and (7), the total strain ε_{ij} can be written in the following form:

$$\varepsilon_{ij} = E^{-1}_{ijkl}\sigma_{kl} + \varepsilon^{\mathrm{p}}_{ij} = \overline{E}^{-1}_{ijkl}\bar{\sigma}_{kl} + \varepsilon^{\mathrm{p}}_{ij} \tag{9}$$

By taking the time derivative of Eq. (3), the rate of the total strain, $\dot{\varepsilon}_{ij}$, can be written as

$$\dot{\varepsilon}_{ij} = \dot{\varepsilon}^{\mathrm{e}}_{ij} + \dot{\varepsilon}^{\mathrm{p}}_{ij} \tag{10}$$

where $\dot{\varepsilon}^{\mathrm{e}}_{ij}$ and $\dot{\varepsilon}^{\mathrm{p}}_{ij}$ are the rate of the elastic and plastic strain tensors, respectively.

Analogous to Eq. (9), one can write the following relation in the effective configuration:

$$\dot{\varepsilon}_{ij} = \overline{E}^{-1}_{ijkl}\dot{\bar{\sigma}}_{kl} + \dot{\varepsilon}^{\mathrm{p}}_{ij} \tag{11}$$

However, since E_{ijkl} is a function of φ_{ij}, a similar relation as Eq. (11) cannot be used. Therefore, by taking the time derivative of Eq. (9), one can write $\dot{\varepsilon}_{ij}$ in the damaged configuration as follows:

$$\dot{\varepsilon}_{ij} = E^{-1}_{ijkl}\dot{\sigma}_{kl} + \dot{E}^{-1}_{ijkl}\sigma_{kl} + \dot{\varepsilon}^{\mathrm{p}}_{ij} \tag{12}$$

Concrete has distinct behavior in tension and compression. Therefore, in order to adequately characterize the damage in concrete due to tensile, compressive, and/or cyclic loadings the Cauchy stress tensor (nominal or effective) is decomposed into a positive and negative parts using the spectral decomposition technique (e.g. Simo and Ju, 1987a,b; Krajcinovic, 1996). Hereafter, the superscripts "+" and "−" designate, respectively, tensile and compressive entities. Therefore, σ_{ij} and $\bar{\sigma}_{ij}$ can be decomposed as follows:

$$\sigma_{ij} = \sigma^+_{ij} + \sigma^-_{ij}, \quad \bar{\sigma}_{ij} = \bar{\sigma}^+_{ij} + \bar{\sigma}^-_{ij} \tag{13}$$

where $\bar{\sigma}^+_{ij}$ is the tension part and $\bar{\sigma}^-_{ij}$ is the compression part of the stress state.

The stress tensors σ^+_{ij} and σ^-_{ij} can be related to σ_{ij} by

$$\sigma^+_{kl} = P^+_{klpq}\sigma_{pq} \tag{14}$$

$$\sigma^-_{kl} = [I_{klpq} - P^+_{ijpq}]\sigma_{pq} = P^-_{klpq}\sigma_{pq} \tag{15}$$

such that $P^{+}_{ijkl} + P^{-}_{ijkl} = I_{ijkl}$. The fourth-order projection tensors P^{+}_{ijkl} and P^{-}_{ijkl} are defined as follows:

$$P^{+}_{ijpq} = \sum_{k=1}^{3} H(\hat{\sigma}^{(k)}) n_i^{(k)} n_j^{(k)} n_p^{(k)} n_q^{(k)}, \quad P^{-}_{klpq} = I_{klpq} - P^{+}_{ijpq} \tag{16}$$

where $H(\hat{\sigma}^{(k)})$ denotes the Heaviside step function computed at kth principal stress $\hat{\sigma}^{(k)}$ of σ_{ij} and $n_i^{(k)}$ is the kth corresponding unit principal direction. In the subsequent development, the superscript hat designates a principal value.

Based on the decomposition in Eq. (13), one can assume that the expression in Eq. (1) to be valid for both tension and compression, however, with decoupled damage evolution in tension and compression such that:

$$\bar{\sigma}^{+}_{ij} = M^{+}_{ijkl}\sigma^{+}_{kl}, \quad \bar{\sigma}^{-}_{ij} = M^{-}_{ijkl}\sigma^{-}_{kl} \tag{17}$$

where M^{+}_{ijkl} is the tensile damage effect tensor and M^{-}_{ijkl} is the corresponding compressive damage effect tensor which can be expressed using Eq. (2) in a decoupled form as a function of the tensile and compressive damage variables, φ^{+}_{ij} and φ^{-}_{ij}, respectively, as follows:

$$M^{+}_{ijkl} = 2[(\delta_{ij} - \varphi^{+}_{ij})\delta_{kl} + \delta_{ij}(\delta_{kl} - \varphi^{+}_{kl})]^{-1}, \quad M^{-}_{ijkl} = 2[(\delta_{ij} - \varphi^{-}_{ij})\delta_{kl} + \delta_{ij}(\delta_{kl} - \varphi^{-}_{kl})]^{-1} \tag{18}$$

Now, by substituting Eq. (17) into Eq. $(13)_2$, one can express the effective stress tensor as the decomposition of the fourth-order damage effect tensor for tension and compression such that:

$$\bar{\sigma}_{ij} = M^{+}_{ijkl}\sigma^{+}_{kl} + M^{-}_{ijkl}\sigma^{-}_{kl} \tag{19}$$

By substituting Eqs. (14) and (15) into Eq. (19) and comparing the result with Eq. (1), one can obtain the following relation for the damage effect tensor such that:

$$M_{ijpq} = M^{+}_{ijkl}P^{+}_{klpq} + M^{-}_{ijkl}P^{-}_{klpq} \tag{20}$$

Using Eq. $(16)_2$, the above equation can be rewritten as follows:

$$M_{ijpq} = \left(M^{+}_{ijkl} - M^{-}_{ijkl}\right)P^{+}_{klpq} + M^{-}_{ijpq} \tag{21}$$

One should notice the following:

$$M_{ijkl} \neq M^{+}_{ijkl} + M^{-}_{ijkl} \tag{22}$$

or

$$\varphi_{ij} \neq \varphi^{+}_{ij} + \varphi^{-}_{ij} \tag{23}$$

It is also noteworthy that the relation in Eq. (21) enhances a coupling between tensile and compressive damage through the fourth-order projection tensor P^{+}_{ijkl}. Moreover, for isotropic damage, Eq. (20) can be written as follows:

$$M_{ijkl} = \frac{P^{+}_{ijkl}}{1 - \varphi^{+}} + \frac{P^{-}_{ijkl}}{1 - \varphi^{-}} \tag{24}$$

It can be concluded from the above expression that by adopting the decomposition of the scalar damage variable φ into a positive φ^{+} part and a negative φ^{-} part still enhances a damage anisotropy through the spectral decomposition tensors P^{+}_{ijkl} and P^{-}_{ijkl}. However, this anisotropy is weak as compared to the anisotropic damage effect tensor presented in Eq. (21).

3. Elasto-plastic-damage model

In this section, the concrete plasticity yield criterion of Lubliner et al. (1989) which was later modified by Lee and Fenves (1998) is adopted for both monotonic and cyclic loadings. The phenomenological concrete model of Lubliner et al. (1989) and Lee and Fenves (1998) is formulated based on isotropic (scalar) stiffness degradation. Moreover, this model adopts one loading surface that couples plasticity to isotropic damage through the effective plastic strain. However, in this work the model of Lee and Fenves (1998) is extended for anisotropic damage and by adopting three loading surfaces: one for plasticity, one for tensile damage, and one for compressive damage. The plasticity and the compressive damage loading surfaces are more dominate in case of shear loading and compressive crushing (i.e. modes II and III cracking) whereas the tensile damage loading surface is dominant in case of mode I cracking.

The presentation in the following sections can be used for either isotropic or anisotropic damage since the second-order damage tensor φ_{ij} degenerates to the scalar damage variable in case of uniaxial loading.

3.1. Uniaxial loading

In the uniaxial loading, the elastic stiffness degradation variables are assumed as increasing functions of the equivalent plastic strains ε^{+}_{eq} and ε^{-}_{eq} with ε^{+}_{eq} being the tensile equivalent plastic strain and ε^{-}_{eq} being the compressive equivalent plastic strain. It should be noted that the material behavior is controlled by both plasticity and damage so that, one cannot be considered without the other (see Fig. 1).

For uniaxial tensile and compressive loading, $\bar{\sigma}^{+}_{ij}$ and $\bar{\sigma}^{-}_{ij}$ are given as (Lee and Fenves, 1998)

$$\sigma^{+} = (1-\varphi^{+})\overline{E}\varepsilon^{+e} = (1-\varphi^{+})\overline{E}(\varepsilon^{+} - \varepsilon^{+p}) \tag{25}$$

$$\sigma^{-} = (1-\varphi^{-})\overline{E}\varepsilon^{-e} = (1-\varphi^{-})\overline{E}(\varepsilon^{-} - \varepsilon^{-p}) \tag{26}$$

The rate of the equivalent (effective) plastic strains in compression and tension, $\varepsilon^{-ep}$and ε^{+ep}, are, respectively, given as follows in case of uniaxial loading:

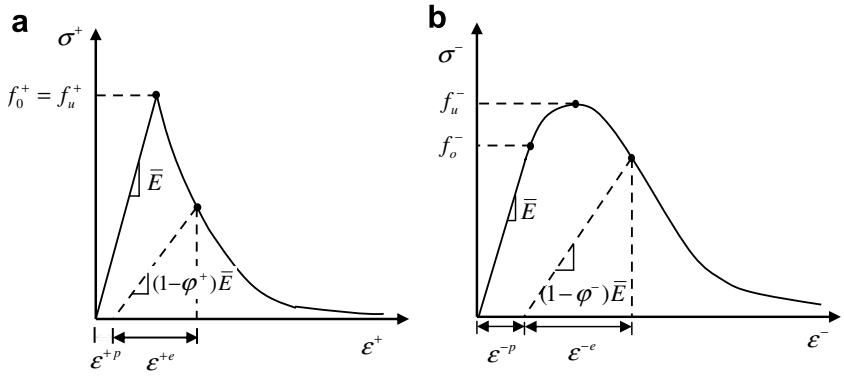

Fig. 1. Concrete behavior under uniaxial (a) tension and (b) compression.

$$\dot{\varepsilon}^{+}_{\mathrm{eq}} = \dot{\varepsilon}^{\mathrm{p}}_{11}, \quad \dot{\varepsilon}^{-}_{\mathrm{eq}} = -\dot{\varepsilon}^{\mathrm{p}}_{11} \tag{27}$$

such that

$$\varepsilon^{-}_{\mathrm{eq}} = \int_0^t \dot{\varepsilon}^{-}_{\mathrm{eq}}\,\mathrm{d}t, \quad \varepsilon^{+}_{\mathrm{eq}} = \int_0^t \dot{\varepsilon}^{+}_{\mathrm{eq}}\,\mathrm{d}t \tag{28}$$

Propagation of cracks under uniaxial loading is in the transverse direction to the stress direction. Therefore, the nucleation and propagation of cracks cause a reduction of the capacity of the load-carrying area, which causes an increase in the effective stress. This has little effect during compressive loading since cracks run parallel to the loading direction. However, under a large compressive stress which causes crushing of the material, the effective load-carrying area is also considerably reduced. This explains the distinct behavior of concrete in tension and compression as shown in Fig. 2.

It can be noted from Fig. 2 that during unloading from any point on the strain softening path (i.e. post peak behavior) of the stress–strain curve, the material response seems to be weakened since the elastic stiffness of the material is degraded due to damage evolution. Furthermore, it can be noticed from Fig. 2a and b that the degradation of the elastic stiffness of the material is much different in tension than in compression, which is more obvious as the plastic strain increases. Therefore, for uniaxial loading, the damage variable can be presented by two independent damage variables φ^{+} and φ^{-}. Moreover, it can be noted that for tensile loading, damage and plasticity are initiated when the equivalent applied stress reaches the uniaxial tensile strength f_0^{+} as shown in Fig. 2a whereas under compressive loading, damage is initiated earlier than plasticity. Once the equivalent applied stress reaches f_0^{-} (i.e. when nonlinear behavior starts) damage is initiated, whereas plasticity occurs once f_{u}^{-} is reached. Therefore, generally $f_0^{+} = f_{\mathrm{u}}^{+}$ for tensile loading, but this is not true for compressive loading (i.e. $f_0^{-} \neq f_{\mathrm{u}}^{-}$). However, one may obtain $f_0^{-} \approx f_{\mathrm{u}}^{-}$ in case of ultra-high strength concrete.

3.2. Multiaxial loading

The evolution equations for the hardening variables are extended now to multiaxial loadings. The effective plastic strain for multiaxial loading is given as follows (Lubliner et al., 1989; Lee and Fenves, 1998):

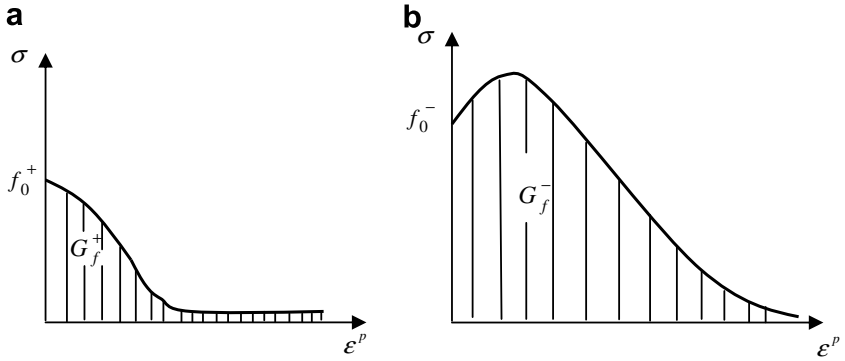

Fig. 2. Schematic representation of the fracture energy under the uniaxial stress–plastic strain diagrams for (a) tension and (b) compression.

$$\dot{\varepsilon}^{+}_{\mathrm{eq}} = r(\hat{\bar{\sigma}}_{ij})\hat{\dot{\varepsilon}}^{\mathrm{p}}_{\mathrm{max}} \tag{29}$$

$$\dot{\varepsilon}^{-}_{\mathrm{eq}} = -(1 - r(\hat{\bar{\sigma}}_{ij}))\hat{\dot{\varepsilon}}^{\mathrm{p}}_{\mathrm{min}} \tag{30}$$

where $\hat{\dot{\varepsilon}}^{\mathrm{p}}_{\mathrm{max}}$ and $\hat{\dot{\varepsilon}}^{\mathrm{p}}_{\mathrm{min}}$ are the maximum and minimum principal values of the plastic strain tensor $\dot{\varepsilon}^{\mathrm{p}}_{ij}$ such that $\hat{\dot{\varepsilon}}^{\mathrm{p}}_{1} > \hat{\dot{\varepsilon}}^{\mathrm{p}}_{2} > \hat{\dot{\varepsilon}}^{\mathrm{p}}_{3}$ where $\hat{\dot{\varepsilon}}^{\mathrm{p}}_{\mathrm{max}} = \hat{\dot{\varepsilon}}^{\mathrm{p}}_{1}$ and $\hat{\dot{\varepsilon}}^{\mathrm{p}}_{\mathrm{min}} = \hat{\dot{\varepsilon}}^{\mathrm{p}}_{3}$.

Eqs. (29) and (30) can be written in tensor format as follows:

$$\dot{\kappa}^{\mathrm{p}}_{i} = H_{ij}\hat{\dot{\varepsilon}}^{\mathrm{p}}_{j} \tag{31}$$

or equivalently

$$\begin{Bmatrix} \dot{\varepsilon}^{+}_{\mathrm{eq}} \\ 0 \\ \dot{\varepsilon}^{-}_{\mathrm{eq}} \end{Bmatrix} = \begin{bmatrix} H^{+} & 0 & 0 \\ 0 & 0 & 0 \\ 0 & 0 & H^{-} \end{bmatrix} \begin{Bmatrix} \hat{\dot{\varepsilon}}^{\mathrm{p}}_{1} \\ \hat{\dot{\varepsilon}}^{\mathrm{p}}_{2} \\ \hat{\dot{\varepsilon}}^{\mathrm{p}}_{3} \end{Bmatrix} \tag{32}$$

where

$$H^{+} = r(\hat{\bar{\sigma}}_{ij}) \tag{33}$$

$$H^{-} = -(1 - r(\hat{\bar{\sigma}}_{ij})) \tag{34}$$

The dimensionless parameter $r(\hat{\bar{\sigma}}_{ij})$ is a weight factor depending on principal stresses and is defined as follows (Lubliner et al., 1989):

$$r(\hat{\bar{\sigma}}_{ij}) = \frac{\sum_{k=1}^{3}\langle\hat{\bar{\sigma}}_{k}\rangle}{\sum_{k=1}^{3}|\hat{\bar{\sigma}}_{k}|} \tag{35}$$

where $\langle\,\rangle$ is the Macauley bracket, and presented as $\langle x\rangle = \frac{1}{2}(|x| + x)$, $k = 1, 2, 3$. Note that $r(\hat{\bar{\sigma}}_{ij}) = r(\hat{\sigma}_{ij})$. Moreover, depending on the value of $r(\hat{\sigma}_{ij})$,

– in case of uniaxial tension $\hat{\bar{\sigma}}_{k} \geqslant 0$ and $r(\hat{\bar{\sigma}}_{ij}) = 1$,
– in case of uniaxial compression $\hat{\bar{\sigma}}_{k} \leqslant 0$ and $r(\hat{\bar{\sigma}}_{ij}) = 0$

3.3. Cyclic loading

It is more difficult to address the concrete damage behavior under cyclic loading; i.e. transition from tension to compression or vise versa such that one would expect that under cyclic loading crack opening and closure may occur and, therefore, it is a challenging task to address such situations especially for anisotropic damage evolution. Experimentally, it is shown that under cyclic loading the material goes through some recovery of the elastic stiffness as the load changes sign during the loading process. This effect becomes more significant particularly when the load changes sign during the transition from tension to compression such that some tensile cracks tend to close and as a result elastic stiffness recovery occurs during compressive loading. However, in case of transition from compression to tension one may thus expect that smaller stiffness recovery or even no recovery at all may occur. This could be attributed to the fast opening of the pre-existing cracks that had formed during the previous tensile loading. These re-opened cracks along with the new cracks formed during the compression will cause further reduction of the elastic stiffness that the body had during the first transition from tension to compression. The

consideration of stiffness recovery effect due to crack opening/closing is therefore important in defining the concrete behavior under cyclic loading. Eq. (21) does not incorporate the elastic stiffness recovery phenomenon as well as it does not incorporate any coupling between tensile damage and compressive damage and, therefore, the formulation of Lee and Fenves (1998) for cyclic loading is extended here for the anisotropic damage case.

Lee and Fenves (1998) defined the following isotropic damage relation that couples both tension and compression effects as well as the elastic stiffness recovery during transition from tension to compression loading such that:

$$\varphi = 1 - (1 - s\varphi^{+})(1 - \varphi^{-}) \tag{36}$$

where $s(0 \leqslant s \leqslant 1)$ is a function of stress state and is defined as follows:

$$s(\hat{\bar{\sigma}}_{ij}) = s_0 + (1 - s_0) r(\hat{\bar{\sigma}}_{ij}) \tag{37}$$

where $0 \leqslant s_0 \leqslant 1$ is a constant. Any value between zero and one results in partial recovery of the elastic stiffness. Based on Eqs. (36) and (37):

(a) when all principal stresses are positive then $r = 1$ and $s = 1$ such that Eq. (36) becomes

$$\varphi = 1 - (1 - \varphi^{+})(1 - \varphi^{-}) \tag{38}$$

which implies no stiffness recovery during the transition from compression to tension since s is absent.

(b) when all principal stresses are negative then $r = 0$ and $s = s_0$ such that Eq. (36) becomes

$$\varphi = 1 - (1 - s_0\varphi^{+})(1 - \varphi^{-}) \tag{39}$$

which implies full elastic stiffness recovery when $s_0 = 0$ and no recovery when $s_0 = 1$.

In the following two approaches are proposed for extending the Lee and Fenves (1998) model to the anisotropic damage case. The first approach is by multiplying φ_{ij}^{+} in Eq. $(18)_1$ by the stiffness recovery factor s:

$$M_{ijkl}^{+} = 2[(\delta_{ij} - s\varphi_{ij}^{+})\delta_{kl} + \delta_{ij}(\delta_{kl} - s\varphi_{kl}^{+})]^{-1} \tag{40}$$

such that the above expression replaces M_{ijkl}^{+} in Eq. (21) to give the total damage effect tensor.

Another approach to enhance coupling between tensile damage and compressive damage as well as in order to incorporate the elastic stiffness recovery during cyclic loading for the anisotropic damage case is by rewriting Eq. (36) in a tensor format as follows:

$$\varphi_{ij} = \delta_{ij} - (\delta_{ik} - s\varphi_{ik}^{+})(\delta_{jk} - \varphi_{jk}^{-}) \tag{41}$$

which can be substituted back into Eq. (2) to get the final form of the damage effect tensor, which is shown next.

It is noteworthy that in case of full elastic stiffness recovery (i.e. $s = 0$), Eq. (41) reduces to $\varphi_{ij} = \varphi_{ij}^{-}$ and in case of no stiffness recovery (i.e. $s = 1$), Eq. (41) takes the form of $\varphi_{ij} = \varphi_{ij}^{-} + \varphi_{ik}^{+} - \varphi_{ik}^{+}\varphi_{jk}^{-}$ such that both φ_{ij}^{+} and φ_{ij}^{-} are coupled. This means that during the transition from tension to compression some cracks are closed or partially closed which could result in partial recovery of the material stiffness (i.e. $s > 0$) in the absence

of damage healing mechanisms. However, during transition from compression to tension, the existing and generated cracks during compressive loading could grow more which causes further stiffness degradation and such that no stiffness recovery is expected. This is why the parameter s only affects the tensile damage variable φ_{ij}^{+}. However, one may argue that during tensile loading a minimal stiffness recovery could occur due to geometrical constraints set up by the interaction between the cracks and the microstructure of concrete. This is what is suggested in the theory manuals of ABAQUS (2003) for the implemented plastic-damage (isotropic) model of Lubliner et al. (1989). However, the former approach is followed in this work where elastic stiffness recovery occurs only during the transition from tensile to compressive state of stress.

Now from Eq. (1), one can write the following:

$$\sigma_{ij} = M_{ijkl}^{-1}\bar{\sigma}_{kl} \tag{42}$$

where M_{ijkl}^{-1} can be written from Eq. (2) as follows:

$$M_{ijkl}^{-1} = \frac{1}{2}[(\delta_{ij} - \varphi_{ij})\delta_{kl} + \delta_{ij}(\delta_{kl} - \varphi_{kl})] \tag{43}$$

By substituting Eq. (41) into Eq. (43), one gets a coupled damage effect tensor in terms of φ_{ij}^{-} and φ_{ij}^{+} as follows:

$$M_{ijkl}^{-1} = \frac{1}{2}[(\delta_{im} - s\varphi_{im}^{+})(\delta_{jm} - \varphi_{jm}^{-})\delta_{kl} + \delta_{ij}(\delta_{km} - s\varphi_{km}^{+})(\delta_{lm} - \varphi_{lm}^{-})] \tag{44}$$

It can be noted that the above expression couples tensile damage and compressive damage. Moreover, it takes into account the stiffness recovery during the transition from tension to compression. For full elastic stiffness recovery ($s = 0$), Eq. (44) yields Eq. $(18)_2$ such that $M_{ijkl} = M_{ijkl}^{-}$. However, for no elastic stiffness recovery ($s = 1$), Eq. (44) reduces to

$$M_{ijkl}^{-1} = \frac{1}{2}[(\delta_{im} - \varphi_{im}^{+})(\delta_{jm} - \varphi_{jm}^{-})\delta_{kl} + \delta_{ij}(\delta_{km} - \varphi_{km}^{+})(\delta_{lm} - \varphi_{lm}^{-})] \tag{45}$$

which shows a coupling between tensile damage and compressive damage.

3.4. Plasticity yield surface

For the representation of concrete behavior under tensile and compressive loadings, a yield criterion is necessary. It is known that concrete behaves differently in tension and compression, thus, the plasticity yield criterion cannot be assumed to be similar. Assuming the same yield criterion for both tension and compression for concrete materials can lead to over/under estimation of plastic deformation (Lubliner et al., 1989). The yield criterion of Lubliner et al. (1989) that accounts for both tension and compression plasticity is adopted in this work. This criterion has been successful in simulating the concrete behavior under uniaxial, biaxial, multiaxial, and cyclic loadings (Lee and Fenves, 1998 and the references outlined there). This criterion is expressed here in the effective (undamaged) configuration and is given as follows:

$$f = \sqrt{3\overline{J}_2} + \alpha\overline{I}_1 + \beta(\kappa_i^{\mathrm{p}})H(\hat{\bar{\sigma}}_{\max})\hat{\bar{\sigma}}_{\max} - (1-\alpha)\dot{c}^{-}(\varepsilon_{\mathrm{eq}}^{-}) \leqslant 0 \tag{46}$$

where $\overline{J}_2 = \bar{s}_{ij}\bar{s}_{ij}/2$ is the second-invariant of the effective deviatoric stress $\bar{s}_{ij} = \bar{\sigma}_{ij} - \bar{\sigma}_{kk}\delta_{ij}/3$, $\overline{I}_1 = \bar{\sigma}_{kk}$ is the first-invariant of the effective stress $\bar{\sigma}_{ij}$, $\kappa_i^{\mathrm{p}} = \int_0^t \dot{\kappa}_i^{\mathrm{p}} dt$ is

the equivalent plastic strain which is defined in Eq. (31), $H(\hat{\bar{\sigma}}_{\max})$ is the Heaviside step function ($H = 1$ for $\hat{\bar{\sigma}}_{\max} > 0$ and H=0 for $\hat{\bar{\sigma}}_{\max} < 0$), and $\hat{\bar{\sigma}}_{\max}$ is the maximum principal stress.

The parameters α and β are dimensionless constants which are defined by Lubliner et al. (1989) as follows:

$$\alpha = \frac{(f_{b0}/f_0^-) - 1}{2(f_{b0}/f_0^-) - 1} \tag{47}$$

$$\beta = (1-\alpha)\frac{c^-(\varepsilon_{\text{eq}}^-)}{c^+(\varepsilon_{\text{eq}}^+)} - (1+\alpha) \tag{48}$$

where f_{b0} and f_0^- are the initial equibiaxial and uniaxial compressive yield stresses, respectively. Experimental values for f_{b0}/f_0^- lie between 1.10 and 1.16; yielding α between 0.08 and 0.12. For more details about the derivation of both Eqs. (47) and (48), the reader is referred to Lubliner et al. (1989).

Since the concrete behavior in compression is more of a ductile behavior, the evolution of the compressive isotropic hardening function $\dot{c}^-$ is defined by the following exponential law:

$$\dot{c}^- = b(Q - c^-)\dot{\varepsilon}_{\text{eq}}^- \tag{49}$$

where Q and b are material constants characterizing the saturated stress and the rate of saturation, respectively, which are obtained in the effective configuration of the compressive uniaxial stress–strain diagram. However, a linear expression is assumed for the evolution of the tensile hardening function $\dot{c}^+$ such that:

$$\dot{c}^+ = h\dot{\varepsilon}_{\text{eq}}^+ \tag{50}$$

where h is a material constant obtained in the effective configuration of the tensile uniaxial stress–strain diagram.

3.5. Non-associative plasticity flow rule

The shape of the concrete loading surface at any given point in a given loading state should be obtained by using a non-associative plasticity flow rule. This is important for realistic modeling of the volumetric expansion under compression for frictional materials such as concrete. Basically, flow rule connects the loading surface and the stress–strain relation. When the current yield surface f is reached, the material is considered to be in plastic flow state upon increase of the loading. In the present model, the flow rule is given as a function of the effective stress $\bar{\sigma}_{ij}$ by

$$\dot{\varepsilon}_{ij}^{\text{p}} = \dot{\lambda}^{\text{p}}\frac{\partial F^{\text{p}}}{\partial \bar{\sigma}_{ij}} \tag{51}$$

where $\dot{\lambda}^{\text{p}}$ is the plastic loading factor or known as the Lagrangian plasticity multiplier, which can be obtained using the plasticity consistency condition, $\dot{f} = 0$, such that

$$f \leqslant 0, \quad \dot{\lambda}^{\text{p}} \geqslant 0, \quad \dot{\lambda}^{\text{p}} f = 0, \quad \dot{\lambda}^{\text{p}}\dot{f} = 0 \tag{52}$$

The plastic potential F^{p} is different than the yield function f (i.e. non-associated) and, therefore, the direction of the plastic flow $\partial F^{\text{p}}/\partial\bar{\sigma}_{ij}$ is not normal to f. One can adopt the Drucker–Prager function for F^{p} such that:

$$F^{\mathrm{p}} = \sqrt{3\bar{J}_2} + \alpha^{\mathrm{p}}\bar{I}_1 \tag{53}$$

where α^{p} is the dilation constant. Then the plastic flow direction $\partial F^{\mathrm{p}}/\partial\bar{\sigma}_{ij}$ is given by

$$\frac{\partial F^{\mathrm{p}}}{\partial\bar{\sigma}_{ij}} = \frac{3}{2}\frac{\bar{s}_{ij}}{\sqrt{3\bar{J}_2}} + \alpha^{\mathrm{p}}\delta_{ij} \tag{54}$$

3.6. Tensile and compressive damage surfaces

The anisotropic damage growth function proposed by Chow and Wang (1987) is adopted in this study. However, this function is generalized here in order to incorporate both tensile and compressive damage separately such that:

$$g^{\pm} = \sqrt{\frac{1}{2}Y^{\pm}_{ij}L^{\pm}_{ijkl}Y^{\pm}_{ij}} - K^{\pm}(\varphi^{\pm}_{\mathrm{eq}}) \leqslant 0 \tag{55}$$

where the superscript $\pm$ designates tension, $+$, or compression, $-$, $K^{\pm}$ is the tensile or compressive damage isotropic hardening function, $K^{\pm} = K^{\pm}_0$ when there is no damage, $K^{\pm}_0$ is the tensile or compressive initial damage parameter (i.e. damage threshold), L_{ijkl} is a fourth-order symmetric tensor, and Y_{ij} is the damage driving force that characterizes damage evolution and is interpreted here as the energy release rate (e.g. Voyiadjis and Kattan, 1992a,b, 1999; Abu Al-Rub and Voyiadjis, 2003; Voyiadjis et al., 2003, 2004). In order to simplify the anisotropic damage formulation, L_{ijkl} is taken in this work as the fourth-order identity tensor I_{ijkl}.

The rate of the equivalent damage $\dot{\varphi}^{\pm}_{\mathrm{eq}}$ is defined as follows (Voyiadjis and Kattan, 1992a,b, 1999; Abu Al-Rub and Voyiadjis, 2003; Voyiadjis et al., 2003, 2004):

$$\dot{\varphi}^{\pm}_{\mathrm{eq}} = \sqrt{\dot{\varphi}^{\pm}_{ij}\dot{\varphi}^{\pm}_{ij}} \quad \text{with} \quad \varphi^{\pm}_{\mathrm{eq}} = \int_0^t \dot{\varphi}^{\pm}_{\mathrm{eq}}\mathrm{d}t \tag{56}$$

The evolution of the tensile damage isotropic hardening function K^{+} is assumed to have the following expression (Mazars and Pijaudier-Cabot, 1989):

$$\dot{K}^{+} = \frac{K^{+}}{B^{+} + \frac{K^{+}_0}{K^{+}}}\exp[-B^{+}(1 - \frac{K^{+}}{K^{+}_0})]\dot{\varphi}^{+}_{\mathrm{eq}} \tag{57}$$

whereas the evolution of the compressive damage isotropic hardening function K^{-} is assumed to have a slightly different form (Mazars and Pijaudier-Cabot, 1989):

$$\dot{K}^{-} = \frac{K^{-}_0}{B^{-}}\exp\left[-B^{-}\left(1 - \frac{K^{-}}{K^{-}_0}\right)\right]\dot{\varphi}^{-}_{\mathrm{eq}} \tag{58}$$

where $K^{\pm}_0$ is the damage threshold which is interpreted as the area under the linear portion of the stress–strain diagram such that:

$$K^{\pm}_0 = \frac{f^{\pm 2}_0}{2\overline{E}} \tag{59}$$

The material constant $B^{\pm}$ is related to the fracture energy $G^{\pm}_f$, which is shown in Fig. 2 for both tension and compression, as follows (Onate et al., 1988):

$$B^{\pm} = \left[\frac{G^{\pm}_f\overline{E}}{\ell f^{\pm 2}_0} - \frac{1}{2}\right]^{-1} \geqslant 0 \tag{60}$$

where ℓ is a characteristic length scale parameter that usually has a value close to the size of the smallest element in a finite element mesh. Of course, a local constitutive model with strain softening (localization) cannot provide an objective description of localized damage and needs to be adjusted or regularized (see Voyiadjis et al., 2004). As a remedy, one may use a simple approach with adjustment of the damage law (which controls softening) according to the size of the finite element, ℓ, in the spirit of the traditional crack-band theory (Bazant and Kim, 1979). Therefore, the parameters $B^{\pm}$ are used to obtain mesh-independent results. A more sophisticated remedy is provided by a localization limiter based on weighted spatial averaging of the damage variable, which will be presented in a forthcoming paper by the authors.

The model response in the damage domain is characterized by the Kuhn–Tucker complementary conditions as follows:

$$g^{\pm} \leqslant 0, \quad \dot{\lambda}_{\mathrm{d}}^{\pm} g^{\pm} = 0, \quad \text{and} \quad \dot{g}^{\pm} \begin{cases} < 0 \Rightarrow \dot{\lambda}_{\mathrm{d}}^{\pm} = 0 \\ = 0 \Rightarrow \dot{\lambda}_{\mathrm{d}}^{\pm} = 0 \\ = 0 \Rightarrow \dot{\lambda}_{\mathrm{d}}^{\pm} > 0 \end{cases} \Longleftrightarrow \begin{cases} \text{effective (undamaged state)} \\ \text{damage initiation} \\ \text{damagegrowth} \end{cases} \tag{61}$$

With the consideration of the above equation, one writes specific conditions for tensile and compressive stages: when $g^{+} < 0$ there is no tensile damage and if $g^{+} > 0$ there is tensile damage in the material; and when $g^{-} < 0$ there is no compressive damage in the material and if $g^{-} > 0$, it means there is compressive damage.

4. Consistent thermodynamic formulation

In this section, the thermodynamic admissibility of the proposed elasto-plastic-damage model is checked following the internal variable procedure of Coleman and Gurtin (1967). The constitutive equations listed in the previous section are derived from the second law of thermodynamics, the expression of Helmholtz free energy, the additive decomposition of the total strain rate in to elastic and plastic components, the Clausius–Duhem inequality, and the maximum dissipation principle.

4.1. Thermodynamic laws

The Helmholtz free energy can be expressed in terms of a suitable set of internal state variables that characterize the elastic, plastic, and damage behavior of concrete. In this work the following internal variables are assumed to satisfactory characterize the concrete behavior both in tension and compression such that:

$$\psi = \psi(\varepsilon_{ij}^{\mathrm{e}}, \varphi_{ij}^{+}, \varphi_{ij}^{-}, \varphi_{\mathrm{eq}}^{+}, \varphi_{\mathrm{eq}}^{-}, \varepsilon_{\mathrm{eq}}^{+}, \varepsilon_{\mathrm{eq}}^{-}) \tag{62}$$

where $\varphi_{\mathrm{eq}}^{+}$ and $\varphi_{\mathrm{eq}}^{-}$ are the equivalent (accumulated) damage variables for tension and compression, respectively, which are defined as $\varphi_{\mathrm{eq}}^{\pm} = \int_0^t \dot{\varphi}_{\mathrm{eq}}^{\pm}\,\mathrm{d}t$. Similarly, $\varepsilon_{\mathrm{eq}}^{+}$ and $\varepsilon_{\mathrm{eq}}^{-}$ are the equivalent tensile and compressive plastic strains that are used here to characterize the plasticity isotropic hardening, $\varepsilon_{\mathrm{eq}}^{\pm} = \int_0^t \dot{\varepsilon}_{\mathrm{eq}}^{\pm}\mathrm{d}t$.

One may argue that it is enough to incorporate the damage tensor $\varphi_{ij}^{\pm}$ instead of incorporating both $\varphi_{ij}^{\pm}$ and $\varphi_{\mathrm{eq}}^{\pm}$. However, the second-order tensor $\varphi_{ij}^{\pm}$ introduces anisotropy while the scalar variable $\varphi_{\mathrm{eq}}^{\pm}$ introduces isotropy characterized by additional hardening.

The Helmholtz free energy is given as a decomposition of elastic, ψ^{e}, plastic, ψ^{p}, and damage, ψ^{d}, parts such that:

$$\psi = \psi^{e}(\varepsilon^{e}_{ij}, \varphi^{+}_{ij}, \varphi^{-}_{ij}) + \psi^{p}(\varepsilon^{+}_{eq}, \varepsilon^{-}_{eq}) + \psi^{d}(\varphi^{+}_{eq}, \varphi^{-}_{eq}) \tag{63}$$

It can be noted from the above decomposition that damage affects only the elastic properties and not the plastic ones. However, for more realistic description, one should introduce the damage variables in the plastic part of the Helmholtz free energy (see Abu Al-Rub and Voyiadjis, 2003; Voyiadjis et al., 2003, 2004). However, these effects are not significant for brittle materials and can, therefore, be neglected.

The elastic free energy ψ^{e} is given in term of the second-order damage tensors $\varphi^{\pm}_{ij}$ as follows:

$$\psi^{e} = \frac{1}{2}\varepsilon^{e}_{ij}E_{ijkl}(\varphi^{+}_{ij}, \varphi^{-}_{ij})\varepsilon^{e}_{kl} = \frac{1}{2}\sigma_{ij}\varepsilon^{e}_{ij} = \frac{1}{2}(\sigma^{+}_{ij} + \sigma^{-}_{ij})\varepsilon^{e}_{ij} \tag{64}$$

Substituting Eq. (17) along with Eqs. (1) and (20), considering $\bar{\sigma}^{+}_{ij} = P^{+}_{ijkl}\bar{\sigma}_{kl}$ and $\bar{\sigma}^{-}_{ij} = P^{-}_{ijkl}\bar{\sigma}_{kl}$ into Eq. (64) and making some algebraic simplifications, one obtains the following relation:

$$\psi^{e} = \frac{1}{2}M^{-1}_{ijpq}\bar{\sigma}_{pq}\varepsilon^{e}_{ij} = \frac{1}{2}\sigma_{ij}\varepsilon^{e}_{ij} \tag{65}$$

such that one can relate the nominal stress to the effective stress through Eq. (42) with M^{-1}_{ijkl} given by

$$M^{-1}_{ijpq} = M^{+^{-1}}_{ijkl}P^{+}_{klpq} + M^{-^{-1}}_{ijkl}P^{-}_{klpq} \tag{66}$$

This suggests that the inverse of Eq. (66) yields Eq. (20) if the projection tensors P^{+}_{klpq} and P^{-}_{klpq} from the effective stress $\bar{\sigma}_{ij}$ coincide with that from the nominal stress σ_{ij}, which is not necessarily true for anisotropic damage. Similarly, for isotropic damage, one can write Eq. (66) as follows:

$$M^{-1}_{ijkl} = (1 - \varphi^{+})P^{+}_{ijkl} + (1 - \varphi^{-})P^{-}_{ijkl} \tag{67}$$

The Clausius–Duhem inequality for isothermal case is given as follows:

$$\sigma_{ij}\dot{\varepsilon}_{ij} - \rho\dot{\psi} \geqslant 0 \tag{68}$$

where ρ is the material density. Taking the time derivative of Eq. (63), the following expression can be written as:

$$\dot{\psi} = \frac{\partial\psi^{e}}{\partial\varepsilon^{e}_{ij}}\dot{\varepsilon}^{e}_{ij} + \frac{\partial\psi^{e}}{\partial\varphi^{+}_{ij}}\dot{\varphi}^{+}_{ij} + \frac{\partial\psi^{e}}{\partial\varphi^{-}_{ij}}\dot{\varphi}^{-}_{ij} + \frac{\partial\psi^{p}}{\partial\varepsilon^{+}_{eq}}\dot{\varepsilon}^{+}_{eq} + \frac{\partial\psi^{p}}{\partial\varepsilon^{-}_{eq}}\dot{\varepsilon}^{-}_{eq} + \frac{\partial\psi^{d}}{\partial\varphi^{+}_{eq}}\dot{\varphi}^{+}_{eq} + \frac{\partial\psi^{d}}{\partial\varphi^{-}_{eq}}\dot{\varphi}^{-}_{eq} \tag{69}$$

By plugging the above equation into the Clausius–Duhem inequality, Eq. (68), and making some simplifications, one can obtain the following relations for any admissible states such that:

$$\sigma_{ij} = \rho\frac{\partial\psi^{e}}{\partial\varepsilon^{e}_{ij}} \tag{70}$$

and

$$\sigma_{ij}\dot{\varepsilon}^{p}_{ij} + Y^{+}_{ij}\dot{\varphi}^{+}_{ij} + Y^{-}_{ij}\dot{\varphi}^{-}_{ij} - c^{+}\dot{\varepsilon}^{+}_{eq} - c^{-}\dot{\varepsilon}^{-}_{eq} - K^{+}\dot{\varphi}^{+}_{eq} - K^{-}\dot{\varphi}^{-}_{eq} \geqslant 0 \tag{71}$$

where the damage and plasticity conjugate forces that appear in the above expression are defined as follows:

$$Y_{ij}^{+} = -\rho \frac{\partial \psi^{e}}{\partial \varphi_{ij}^{+}} \tag{72}$$

$$Y_{ij}^{-} = -\rho \frac{\partial \psi^{e}}{\partial \varphi_{ij}^{-}} \tag{73}$$

$$K^{+} = \rho \frac{\partial \psi^{d}}{\partial \varphi_{eq}^{+}} \tag{74}$$

$$K^{-} = \rho \frac{\partial \psi^{d}}{\partial \varphi_{eq}^{-}} \tag{75}$$

$$c^{+} = \rho \frac{\partial \psi^{p}}{\partial \varepsilon_{eq}^{+}} \tag{76}$$

$$c^{-} = \rho \frac{\partial \psi^{p}}{\partial \varepsilon_{eq}^{-}} \tag{77}$$

Therefore, one can rewrite the Clausius–Duhem inequality to yield the dissipation energy, Π, due to plasticity, Π^{p}, and damage, Π^{d}, such that

$$\Pi = \Pi^{d} + \Pi^{p} \geqslant 0 \tag{78}$$

with

$$\Pi^{p} = \sigma_{ij}\dot{\varepsilon}_{ij}^{p} - c^{+}\dot{\varepsilon}_{eq}^{+} - c^{-}\dot{\varepsilon}_{eq}^{-} \geqslant 0 \tag{79}$$

$$\Pi^{d} = Y_{ij}^{+}\dot{\varphi}_{ij}^{+} + Y_{ij}^{-}\dot{\varphi}_{ij}^{-} - K^{+}\dot{\varphi}_{eq}^{+} - K^{-}\dot{\varphi}_{eq}^{-} \geqslant 0 \tag{80}$$

The rate of the internal variables associated with plastic and damage deformations are obtained by utilizing the calculus of functions of several variables with the plasticity and damage Lagrangian multipliers, $\dot{\lambda}^{p}$ and $\dot{\lambda}_{d}^{\pm}$, such that the following objective function can be defined:

$$\Omega = \Pi - \dot{\lambda}^{p}F^{p} - \dot{\lambda}_{d}^{+}g^{+} - \dot{\lambda}_{d}^{-}g^{-} \geqslant 0 \tag{81}$$

Using the well-known maximum dissipation principle (Simo and Honein, 1990; Simo and Hughes, 1998), which states that the actual state of the thermodynamic forces (σ_{ij}, $Y_{ij}^{\pm}$, $c^{\pm}$, $K^{\pm}$) is that which maximizes the dissipation function over all other possible admissible states, hence, one can maximize the objective function Ω by using the necessary conditions as follows:

$$\frac{\partial \Omega}{\partial \sigma_{ij}} = 0, \quad \frac{\partial \Omega}{\partial Y_{ij}^{\pm}} = 0, \quad \frac{\partial \Omega}{\partial c^{\pm}} = 0, \quad \frac{\partial \Omega}{\partial K^{\pm}} = 0 \tag{82}$$

Substituting Eq. (81) along with Eqs. (79) and (80) into Eq. (82) yield the following thermodynamic laws:

$$\dot{\varepsilon}_{ij}^{p} = \dot{\lambda}^{p}\frac{\partial F^{p}}{\partial \sigma_{ij}} \tag{83}$$

$$\dot{\varphi}_{ij}^{+} = \dot{\lambda}_{d}^{+}\frac{\partial g^{+}}{\partial Y_{ij}^{+}} \tag{84}$$

$$\dot{\varphi}_{ij}^{-} = \dot{\lambda}_{\mathrm{d}}^{-} \frac{\partial g^{-}}{\partial Y_{ij}^{-}} \tag{85}$$

$$\dot{\varepsilon}_{\mathrm{eq}}^{+} = \dot{\lambda}^{\mathrm{p}} \frac{\partial F^{\mathrm{p}}}{\partial c^{+}} \tag{86}$$

$$\dot{\varepsilon}_{\mathrm{eq}}^{-} = \dot{\lambda}^{\mathrm{p}} \frac{\partial F^{\mathrm{p}}}{\partial c^{-}} \tag{87}$$

$$\dot{\varphi}_{\mathrm{eq}}^{+} = \dot{\lambda}_{\mathrm{d}}^{+} \frac{\partial g^{+}}{\partial K^{+}} \tag{88}$$

$$\dot{\varphi}_{\mathrm{eq}}^{-} = \dot{\lambda}_{\mathrm{d}}^{-} \frac{\partial g^{-}}{\partial K^{-}} \tag{89}$$

4.2. The Helmholtz free energy function

The elastic part of the Helmholtz free energy function, ψ^{e}, as presented in Eq. (64) can be substituted into Eq. (70) to yield the following stress–strain relation:

$$\sigma_{ij} = E_{ijkl}\varepsilon_{kl}^{\mathrm{e}} = E_{ijkl}(\varepsilon_{kl} - \varepsilon_{kl}^{\mathrm{p}}) \tag{90}$$

Now, one can obtain expressions for the damage driving forces $Y_{ij}^{\pm}$ from Eqs. (64), (72), and (73) as follows:

$$Y_{rs}^{\pm} = -\frac{1}{2}\varepsilon_{ij}^{\mathrm{e}} \frac{\partial E_{ijkl}}{\partial \varphi_{rs}^{\pm}} \varepsilon_{kl}^{\mathrm{e}} \tag{91}$$

By taking the derivative of Eq. (8) with respect to the damage parameter $\varphi_{ij}^{\pm}$ one obtains

$$\frac{\partial E_{ijkl}}{\partial \varphi_{rs}^{\pm}} = \frac{\partial M_{ijmn}^{-1}}{\partial \varphi_{rs}^{\pm}} \overline{E}_{mnkl} \tag{92}$$

Now, by substituting Eq. (92) into Eq. (91), one obtains the following expression for $Y_{ij}^{\pm}$:

$$Y_{rs}^{\pm} = -\frac{1}{2}\varepsilon_{ij}^{\mathrm{e}} \frac{\partial M_{ijmn}^{-1}}{\partial \varphi_{rs}^{\pm}} \overline{E}_{mnkl} \varepsilon_{kl}^{\mathrm{e}} \tag{93}$$

where from Eq. (66), one can write the following expression:

$$\frac{\partial M_{ijmn}^{-1}}{\partial \varphi_{rs}^{\pm}} = \frac{\partial M_{ijpq}^{\pm -1}}{\partial \varphi_{rs}^{\pm}} P_{pqmn}^{\pm} \tag{94}$$

One can also rewrite Eq. (93) in terms of the effective stress tensor by replacing $\varepsilon_{kl}^{\mathrm{e}}$ from Eq. (4) as follows:

$$Y_{rs}^{\pm} = -\frac{1}{2}\overline{E}_{ijab}^{-1}\bar{\sigma}_{ab} \frac{\partial M_{ijpq}^{-1}}{\partial \varphi_{rs}^{\pm}} \bar{\sigma}_{pq} \tag{95}$$

The plastic part of the Helmholtz free energy function is postulated to have the following form (Abu Al-Rub and Voyiadjis, 2003; Voyiadjis et al., 2003, 2004):

$$\rho\psi^{\mathrm{p}} = f_0^{+}\varepsilon^{+ep} + \frac{1}{2}h(\varepsilon_{\mathrm{eq}}^{+})^2 + f_0^{-}\varepsilon_{\mathrm{eq}}^{-} + Q\left(\varepsilon_{\mathrm{eq}}^{-} + \frac{1}{b}\exp(-b\varepsilon_{\mathrm{eq}}^{-})\right) \tag{96}$$

Substituting Eq. (96) into Eqs. (82) and (83) yields the following expressions for the plasticity conjugate forces c^+ and c^-:

$$c^+ = f_0^+ + h\varepsilon_{\mathrm{eq}}^+ \tag{97}$$

$$c^- = f_0^- + Q\left[1 - \exp(-b\varepsilon_{\mathrm{eq}}^-)\right] \tag{98}$$

such that by taking the time derivative of Eqs. (97) and (98) one can easily retrieve Eqs. (49) and (50), respectively.

The damage part of the Helmholtz free energy function is postulated to have the following form:

$$\rho\psi^{\mathrm{d}} = K_0^{\pm}[\varphi_{\mathrm{eq}}^{\pm} + \frac{1}{B^{\pm}}\{(1-\varphi_{\mathrm{eq}}^{\pm})\ln(1-\varphi_{\mathrm{eq}}^{\pm}) + \varphi_{\mathrm{eq}}^{\pm}\}] \tag{99}$$

where $K_0^{\pm}$ is the initial damage threshold defined in Eq. (59) and $B^{\pm}$ are material constants which are expressed in terms of the fracture energy and an intrinsic length scale, Eq. (60).

Substituting Eq. (90) into Eqs. (74) and (75), one can easily obtain the following expressions for the damage driving forces $K^{\pm}$:

$$K^{\pm} = K_0^{\pm}[1 - \frac{1}{B^{\pm}}\ln(1-\varphi_{\mathrm{eq}}^{\pm})] \tag{100}$$

By taking the time derivative of the above expression one retrieves the rate form of the damage hardening/softening function $K^{\pm}$ presented in Eqs. (57) and (58) such that:

$$\dot{K}^{\pm} = \frac{K_0^{\pm}}{B^{\pm}}\exp\left[-B^{\pm}(1-\frac{K^{\pm}}{K_0^{\pm}})\right]\dot{\varphi}_{\mathrm{eq}}^{\pm} \tag{101}$$

It is noteworthy that the expression that is presented in Eq. (58) for tensile damage is a slightly different than the one shown in Eq. (101). However, in the remaining of this study, Eq. (57) is used. This is attributed to the better representation of the stress–strain diagram under tensile loading, when Eq. (58) is used instead of Eq. (101).

5. Numerical implementation

In this section, the time discretization and numerical integration procedures are presented. The evolutions of the plastic and damage internal state variables can be obtained if the Lagrangian multipliers $\dot{\lambda}^{\mathrm{p}}$ and $\dot{\lambda}_{\mathrm{d}}^{\pm}$ are computed. The plasticity and damage consistency conditions, Eqs. (52) and (61), are used for computing both $\dot{\lambda}^{\mathrm{p}}$ and $\dot{\lambda}_{\mathrm{d}}^{\pm}$. This is shown in the subsequent developments. Then, by applying the given strain increment $\Delta\varepsilon_{ij} = \varepsilon_{ij}^{(n+1)} - \varepsilon_{ij}^{(n)}$ and knowing the values of the stress and internal variables at the beginning of the step from the previous step, $(\cdot)^{(n)}$, the updated values at the end of the step, $(\cdot)^{(n+1)}$, are obtained.

The implemented integration scheme is divided into two sequential steps, corresponding to the plastic and damage parts of the model. In the plastic part, the plastic strain $\varepsilon_{ij}^{\mathrm{p}}$ and the effective stress $\bar{\sigma}_{ij}$ at the end of the step are determined by using the classical radial return mapping algorithm (Simo and Hughes, 1998) such that:

$$\bar{\sigma}_{ij} = \bar{\sigma}_{ij}^{\mathrm{tr}} - \overline{E}_{ijkl}\Delta\varepsilon_{kl}^{\mathrm{p}} = \bar{\sigma}_{ij}^{\mathrm{tr}} - \Delta\lambda^{\mathrm{p}}\overline{E}_{ijkl}\frac{\partial F^{\mathrm{p}}}{\partial\bar{\sigma}_{kl}^{(n)}} \tag{102}$$

where $\bar{\sigma}_{ij}^{\mathrm{tr}} = \bar{\sigma}_{ij}^{(n)} + \overline{E}_{ijkl}\Delta\varepsilon_{kl}$ is the trial stress tensor, which is easily evaluated from the given strain increment. If the trial stress is not outside the yield surface, i.e. $f(\bar{\sigma}_{ij}^{\mathrm{tr}}, c_c^{(n)}) \leqslant 0$, the step is elastic and one sets $\Delta\lambda^{\mathrm{p}} = 0$, $\bar{\sigma}_{ij}^{\mathrm{tr}} = \bar{\sigma}_{ij}^{(n+1)}$, $\varepsilon_{ij}^{p(n+1)} = \varepsilon_{ij}^{p(n)}$, $c^{\pm(n+1)} = c^{\pm(n)}$. However, if the trial stress is outside the yield surface $\bar{\sigma}_{ij}^{(n+1)}$, $\varepsilon_{ij}^{p(n+1)}$, and $c^{\pm(n+1)}$ are determined by computing $\Delta\lambda^{\mathrm{p}}$.

In the damage part, the nominal stress σ_{ij} at the end of the step is obtained from Eq. (42) by knowing the damage variables $\varphi_{ij}^{\pm}$, which can be calculated once $\Delta\lambda_{\mathrm{d}}^{\pm}$ are computed from the damage consistency conditions.

5.1. Evolution of the plastic multiplier

From the effective consistency condition, one can write the following relation at $n+1$ step:

$$f^{(n+1)} = f^{(n)} + \Delta f \tag{103}$$

where

$$\Delta f = \frac{\partial f}{\partial \bar{\sigma}_{ij}}\Delta\bar{\sigma}_{ij} + \frac{\partial f}{\partial \hat{\bar{\sigma}}_{\max}}\Delta\hat{\bar{\sigma}}_{\max} + \frac{\partial f}{\partial \varepsilon_{\mathrm{eq}}^{-}}\Delta\varepsilon_{\mathrm{eq}}^{-} + \frac{\partial f}{\partial \varepsilon_{\mathrm{eq}}^{+}}\Delta\varepsilon_{\mathrm{eq}}^{+} = 0 \tag{104}$$

$$f^{(n+1)} = \sqrt{3\overline{J}_2^{(n+1)}} + \alpha\overline{I}_1^{(n+1)} - \bar{\beta}^{(n+1)}\hat{\bar{\sigma}}_{\max}^{(n+1)} - (1-\alpha)c^{-(n+1)} = 0 \tag{105}$$

$$\bar{\beta}^{(n+1)} = H(\hat{\bar{\sigma}}_{\max}^{(n+1)})\beta^{(n+1)} \tag{106}$$

Making few arithmetic manipulations, one can obtain the plastic multiplier $\Delta\lambda^{\mathrm{p}}$ from the following expression:

$$\Delta\lambda^{\mathrm{p}} = \frac{f^{\mathrm{tr}}}{H} \tag{107}$$

where f^{tr} and H are given as

$$f^{\mathrm{tr}} = \sqrt{\frac{3}{2}}\|\bar{s}_{ij}^{\mathrm{tr}}\| + \alpha\overline{I}_1^{\mathrm{tr}} - \bar{\beta}\hat{\bar{\sigma}}_{\max}^{\mathrm{tr}} - (1-\alpha)c^{-(n)} \tag{108}$$

$$H = 3\overline{G} + 9\overline{K}\alpha_p\alpha + \bar{\beta}Z + (1-r)\frac{\partial f}{\partial \varepsilon_{\mathrm{eq}}^{-}}\frac{\partial F^{\mathrm{p}}}{\partial \hat{\bar{\sigma}}_{\min}^{\mathrm{tr}}} - r\frac{\partial f}{\partial \varepsilon_{\mathrm{eq}}^{+}}\frac{\partial F^{\mathrm{p}}}{\partial \hat{\bar{\sigma}}_{\max}^{\mathrm{tr}}} \tag{109}$$

with

$$Z = \sqrt{6}\overline{G}\frac{\hat{\bar{\sigma}}_{\max}^{\mathrm{tr}}}{\|\bar{s}_{ij}^{\mathrm{tr}}\|} + 3\overline{K}\alpha_p - \sqrt{\frac{2}{3}}\overline{G}\frac{\overline{I}_1^{\mathrm{tr}}}{\|\bar{s}_{ij}^{\mathrm{tr}}\|} \tag{110}$$

$$\frac{\partial F^{\mathrm{p}}}{\partial \hat{\bar{\sigma}}_{\min,\max}^{\mathrm{tr}}} = \sqrt{\frac{3}{2}}\frac{\left(\hat{\bar{\sigma}}_{\min,\max}^{\mathrm{tr}} - \frac{1}{3}\overline{I}_1^{\mathrm{tr}}\right)}{\|\bar{s}_{ij}^{\mathrm{tr}}\|} + \alpha_p \tag{111}$$

$$\frac{\partial f}{\partial \varepsilon_{\mathrm{eq}}^{-}} = -(1-\alpha)Qb\exp(-b\varepsilon_{\mathrm{eq}}^{-})\left[1 - \frac{\langle\hat{\bar{\sigma}}_{\max}\rangle}{c^{+}}\right] \tag{112}$$

$$\frac{\partial f}{\partial \varepsilon_{\mathrm{eq}}^{+}} = -\langle\hat{\bar{\sigma}}_{\max}\rangle\frac{c^{-}(1-\alpha)h}{(c^{+})^2} \tag{113}$$

It should be noted that, in the case of the Drucker–Prager potential function, a singular region occurs near the cone tip unless $\alpha_p = 0$. The reason of the occurrence of the singular region is that any trial stress that belongs to the singular region cannot be mapped back to a returning point on the given yield surface.

5.2. Evolution of the tensile and compressive damage multipliers

In the following, the damage multipliers, $\dot{\lambda}^{\pm}_{\mathrm{d}}$, are obtained using the consistency conditions in Eq. (61). The incremental expression for the damage consistency condition can be written as

$$g^{\pm(n+1)} = g^{\pm(n)} + \Delta g^{\pm} = 0 \tag{114}$$

where g^{+} is the damage surface function given in Eq. (55) and Δg^{+} is the increment of the tensile damage function which is expressed by

$$\Delta g^{\pm} = \frac{\partial g^{\pm}}{\partial Y^{\pm}_{ij}} \Delta Y^{\pm}_{ij} + \frac{\partial g^{\pm}}{\partial K^{\pm}} \Delta K^{\pm} \tag{115}$$

However, since $Y^{\pm}_{ij}$ is a function of $\sigma^{\pm}_{ij}$ and $\varphi^{\pm}_{ij}$ one can write the following:

$$\Delta Y^{\pm}_{ij} = \frac{\partial Y^{\pm}_{ij}}{\partial \sigma^{\pm}_{kl}} \Delta \sigma^{\pm}_{kl} + \frac{\partial Y^{\pm}_{ij}}{\partial \varphi^{\pm}_{kl}} \Delta \varphi^{\pm}_{kl} \tag{116}$$

where $\Delta\varphi^{\pm}_{kl}$ is obtained from Eqs. (84) and (85) such that:

$$\Delta \varphi^{\pm}_{kl} = \Delta \lambda^{\pm}_{\mathrm{d}} \frac{\partial g^{\pm}}{\partial Y^{\pm}_{kl}} \tag{117}$$

and $\Delta\sigma^{\pm}_{kl}$ can be obtained from Eq. (17) as follows:

$$\Delta \sigma^{\pm}_{kl} = \frac{\partial M^{-1^{\pm}}_{klrs}}{\partial \varphi^{\pm}_{mn}} \Delta \varphi^{\pm}_{mn} \bar{\sigma}^{\pm}_{rs} + M^{-1^{\pm}}_{klrs} \Delta \bar{\sigma}^{\pm}_{rs} \tag{118}$$

By substituting Eqs. (116)–(118) into Eq. (115) and noticing that $\dot{\lambda}^{\pm} = \dot{\varphi}^{\pm}_{\mathrm{eq}} = \sqrt{\dot{\varphi}^{\pm}_{ij}\dot{\varphi}^{\pm}_{ij}}$, one can obtain the following relation:

$$\begin{aligned} \Delta g^{\pm} = {} & \frac{\partial g^{\pm}}{\partial Y^{\pm}_{ij}} \frac{\partial Y^{\pm}_{ij}}{\partial \sigma^{\pm}_{kl}} \frac{\partial M^{-1^{\pm}}_{klrs}}{\partial \varphi^{\pm}_{mn}} \bar{\sigma}^{\pm}_{rs} \frac{\partial g^{\pm}}{\partial Y^{\pm}_{mn}} \Delta \lambda^{\pm}_{\mathrm{d}} + \frac{\partial g^{\pm}}{\partial Y^{\pm}_{ij}} \frac{\partial Y^{\pm}_{ij}}{\partial \sigma^{\pm}_{kl}} M^{-1^{\pm}}_{klrs} \Delta \bar{\sigma}^{\pm}_{rs} + \frac{\partial g^{\pm}}{\partial Y^{\pm}_{ij}} \frac{\partial Y^{\pm}_{ij}}{\partial \varphi^{\pm}_{kl}} \\ & \times \frac{\partial g^{\pm}}{\partial Y^{\pm}_{kl}} \Delta \lambda^{\pm}_{\mathrm{d}} + \frac{\partial g^{\pm}}{\partial K^{\pm}} \frac{\partial K^{\pm}}{\partial \varphi^{\pm}_{\mathrm{eq}}} \Delta \lambda^{\pm}_{\mathrm{d}} \end{aligned} \tag{119}$$

Substituting the above equation into Eq. (114), one obtains $\Delta\lambda^{\pm}_{\mathrm{eq}}$ by the following relation:

$$\Delta \lambda^{\pm}_{\mathrm{eq}} = -\frac{g^{\pm(n)}}{H^{\pm}_{\mathrm{eq}}} \tag{120}$$

where $H^{\pm}_{\mathrm{eq}}$ is the tensile or compressive damage hardening/softening modulus and is given as follows:

$$H^{\pm}_{\mathrm{eq}} = \frac{\partial g^{\pm}}{\partial Y^{\pm}_{ij}} \frac{\partial Y^{\pm}_{ij}}{\partial \sigma^{\pm}_{kl}} \frac{\partial M^{-1^{\pm}}_{klrs}}{\partial \varphi^{\pm}_{mn}} \bar{\sigma}^{\pm}_{rs} \frac{\partial g^{\pm}}{\partial Y^{\pm}_{mn}} + \frac{\partial g^{\pm}}{\partial Y^{\pm}_{ij}} \frac{\partial Y^{\pm}_{ij}}{\partial \varphi^{\pm}_{kl}} \frac{\partial g^{\pm}}{\partial Y^{\pm}_{kl}} + \frac{\partial g^{\pm}}{\partial K^{\pm}} \frac{\partial K^{\pm}}{\partial \varphi^{\pm}_{\mathrm{eq}}} \tag{121}$$

where $\partial g/\partial K = -1$ and the expressions for $\partial g/\partial Y_{ij}$, $\partial Y_{ij}/\partial \sigma_{kl}$, $\partial M^{-1}_{klrs}/\partial \varphi_{mn}$, and $\partial Y_{ij}/\partial \varphi_{kl}$ can be found in Abu Al-Rub and Voyiadjis (2003), Voyiadjis et al. (2003, 2004), whereas the expression of $\partial K/\partial \varphi_{\text{eq}}$ can be obtained from Eq. (100).

It is noteworthy that the consistent (algorithmic) tangent stiffness is used to speed the rate of convergence of the Newton–Raphson method. The expression of this stiffness can be simply obtained using the guidelines in Simo and Hughes (1998).

6. Comparison with experimental results

The use of the present model in solving several problems is conducted using the finite element program, ABAQUS (2003). The proposed constitutive model and the numerical algorithm presented in the previous section are implemented in ABAQUS via the user subroutine UMAT. Comparison of the results is done using experimental data for uniaxial loadings (Karsan and Jirsa, 1969) and biaxial loading (Kupfer et al., 1969) for normal strength of concrete (NSC). The material constants used in conducting these comparisons are listed in Table 1. These material constants are obtained from the experimental results in Fig. 4. The values for $\overline{E}$, ν, f_u^+, f_u^-, α_p, and α are taken from the work of Lee and Fenves (1998). The values for the fracture energies $G_f^{\pm}$ are obtained by establishing the stress-plastic strain diagram and then calculating the area under the curve (see Fig. 2). A material length scale of $\ell = 50$ mm is assumed as a typical measure of the size of the localized damage zone in frictional materials, which is used along with $G_f^{\pm}$ to calculate the damage constants $B^{\pm}$ from Eq. (60). Furthermore, it is assumed that the onset of plasticity, characterized by $f_0^{\pm}$, coincides with the onset of damage, characterized by $K_0^{\pm}$ in Eq. (59), such that $f_0^+ = f_u^+$ whereas f_0^- is obtained from Fig. 4(b) beyond which nonlinearity becomes visible. Generally, h, Q, and b can be obtained by constructing the effective stress, $\bar{\sigma} = \sigma/(1-\varphi_{11})$, versus the plastic strain diagram such that φ_{11} can be obtained by measuring the reduction in the material stiffness from loading/reloading uniaxial cyclic test (one point is extracted for each unloading cycle). However, due to the lack of such experimental data, the material constants h, Q, and b are obtained by taking the best fit of the experimental data in Fig. 4a and b.

A single-element mesh of size 200 × 200 mm and with one Gauss integration point is used in testing the proposed elasto-plastic-damage model (see Fig. 3). Simulations are performed using one step and 100 iterations. Convergence is obtained quickly. Numerical results show a good agreement between the stress–strain curves compared to the experimental results as shown for uniaxial and biaxial tensile/compressive loadings in Figs. 4 and 5, respectively. Although the experimental data in Fig. 4a shows a very steep softening curve, the proposed model can predict to a large extent such a large negative stiffness. The simulated compressive stress–strain curve in Fig. 4b agrees very well with the experimental data.

Table 1
The material constants for normal strength concrete

$\overline{E} = 31.7$ GPa	$\nu = 0.2$	$f_u^+ = 3.48$ MPa	$f_u^- = 27.6$ MPa
$f_0^+ = 3.48$ MPa	$f_0^- = 20$ MPa	$G_f^+ = 42$ N/m	$G_f^- = 1765$ N/m
$\alpha_p = 0.2$	$\alpha = 0.12$	$\ell = 50$ mm	$h = 25$ GPa
$Q = 50$ MPa	$b = 2200$	$B^+ = 0.54$	$B^- = 0.12$
$K_0^+ = 191$ N/m^2	$K_0^- = 6310$ N/m^2		

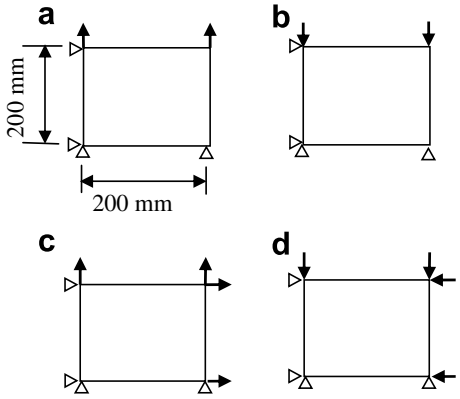

Fig. 3. (a) Uniaxial tension, (b) uniaxial compression, (c) biaxial tension, and (d) biaxial compression.

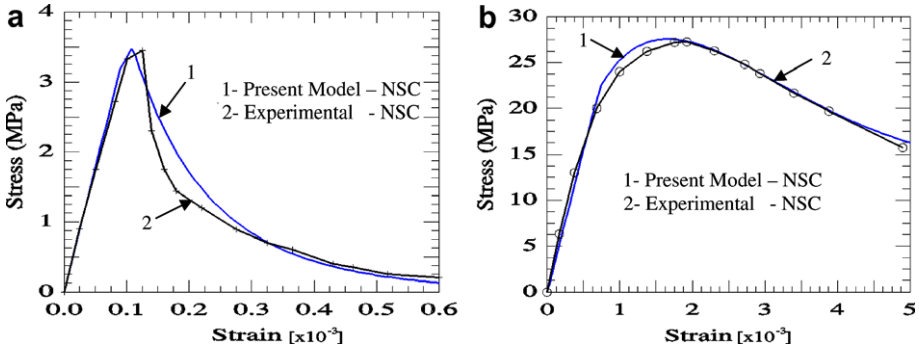

Fig. 4. Stress–strain curves for (a) uniaxial tension and (b) uniaxial compression. Comparison of the model predictions with experimental results (Karsan and Jirsa, 1969).

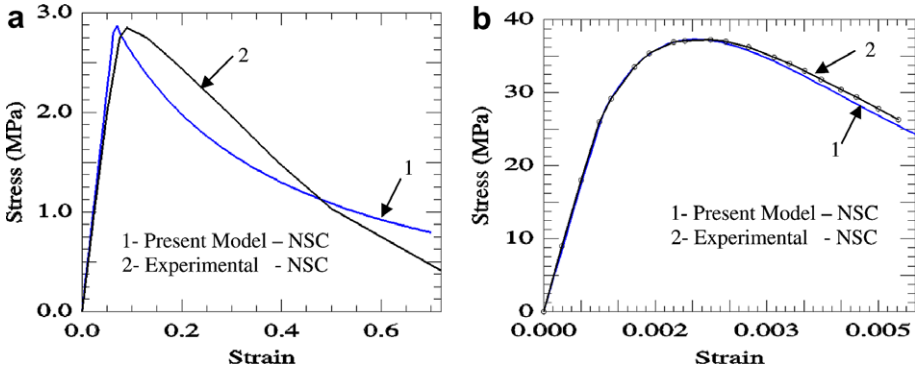

Fig. 5. Stress–strain curves for (a) biaxial tension and (b) biaxial compression. Comparison of the model predictions with experimental results (Kupfer et al., 1969).

The same material constants as listed in Table 1 are used to test the model under biaxial loading. It can be seen that the dilatancy in concrete, which is mainly controlled by the α_p parameter in the plastic potential function, can be modeled well by the present model.

Figs. 6 and 7 show the damage evolution versus strain for the numerical uniaxial and biaxial curves in Figs. 4 and 5. It can be noted from Fig. 6a that the maximum tensile damage is about 0.88 which corresponds to a strain of 0.6×10^{-3}, whereas Fig. 6b shows a maximum compressive damage of 0.62 at a strain of 5×10^{-3}. As expected the material under compressive loading damages less and sustains more load than under tensile loading. Moreover, Fig. 7a shows a maximum biaxial tensile damage of 0.65 at 0.7×10^{-3}, whereas Fig. 7b shows a maximum compression damage of 0.75 at a strain of 7×10^{-3}. This indicates that in biaxial compression the material sustains more strains and as a result of that, higher values of damage occur than in the corresponding biaxial tension.

It is noteworthy to compare the damage evolution in both uniaxial and biaxial tensile/compressive loadings as shown in Fig. 8. It can be seen that the largest evolution of damage occurs during uniaxial tension. Moreover, generally one can conclude that damage evolution during uniaxial tensile loading is higher than biaxial or multiaxial tensile loading. This can be attributed to geometrical constraints set by the evolution of cracks in different directions during biaxial or multiaxial loadings such that crack propagation can be suppressed by other propagating cracks. Interaction between cracks may cause the material to harden such that a stronger response is obtained. However, an interesting behavior

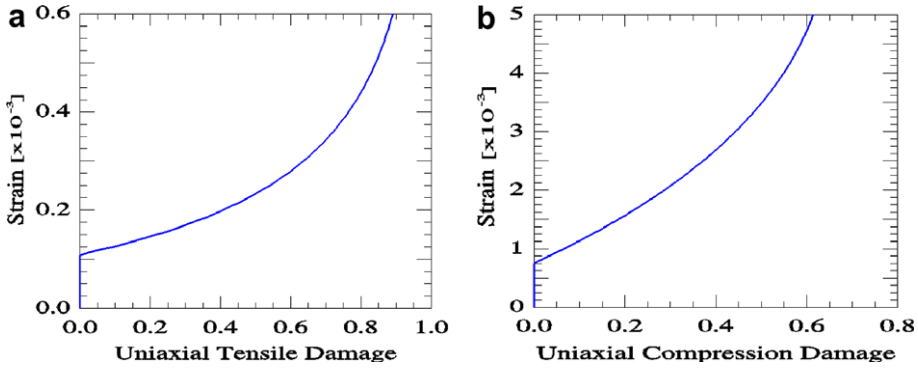

Fig. 6. Damage evolution in (a) uniaxial tension and (b) uniaxial compression.

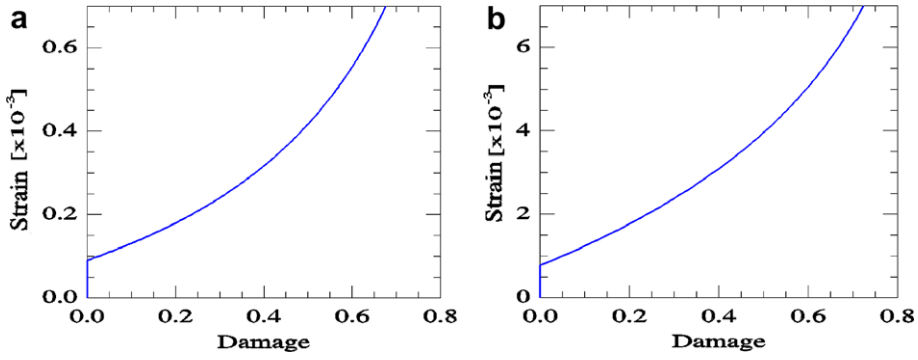

Fig. 7. Damage evolution in (a) biaxial tension and (b) biaxial compression.

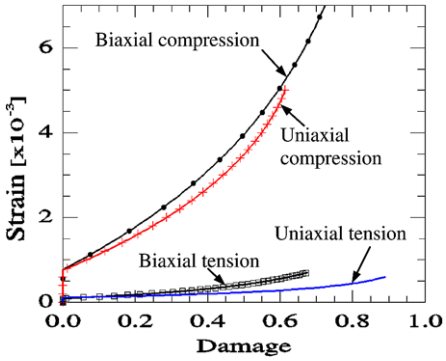

Fig. 8. Comparison between the damage evolution during uniaxial and biaxial tensile and compressive loadings.

can also be noticed such that the previous conclusion cannot be inferred from the evolution of damage during uniaxial and biaxial compression. One can notice from Fig. 8 that the amount of cracks generated during biaxial compression is higher than during uniaxial compression. This can be attributed to the amount of generated dilation and shear cracks (crushing) being larger during biaxial compression.

7. Conclusions

An elasto-plasticity-damage model for plain concrete is presented in this work. Based on continuum damage mechanics, anisotropic damage evolution is considered. The plasticity and damage loading surfaces account for both compressive and tensile loadings such that the tensile and compressive damage are characterized independently. The plasticity yield surface is expressed in the effective (undamaged) configuration, which leads to a decoupled algorithm for the effective stress computation and the damage evolution. The constitutive relations are validated using the second law of thermodynamics. Numerical algorithm is presented for the implementation of the proposed model in the well-known finite element code ABAQUS via the material user subroutine UMAT.

The overall performance of the proposed model is tested by comparing the model predictions to experimental data. Experimental simulations of concrete response under uniaxial and biaxial loadings for both tension and compression show well agreement with the experimental data. This shows that the proposed model with corporation of plasticity and damage provides an effective method for modeling the concrete behavior in tension and compression. The damage evolution for both uniaxial–biaxial and tensile–compressive loadings shows a clear representation of the failure of concrete.

The proposed model can be applied to numerous structural engineering applications. This will be the focus of forthcoming papers by the current authors. Moreover, the presented local constitutive relations result in ill-posed initial boundary value problem for material softening (Voyiadjis et al., 2004). Consequently, uniqueness of the solution for the problem is not guaranteed such that mesh dependent results in the finite element analysis may be obtained. However, to overcome this problem a localization limiter such as the strain gradient theory (Voyiadjis et al., 2004) can be used. This will be presented in detail in a separate publication.

References

ABAQUS. 2003. Version 6.3, Habbitt, Karlsson and Sorensen, Inc., Providence, RI.

Abu Al-Rub, R.K., Voyiadjis, G.Z., 2003. On the coupling of anisotropic damage and plasticity models for ductile materials. International Journal of Solids and Structures 40, 2611–2643.

Abu Al-Rub, R.K., Voyiadjis, G.Z., 2004. Analytical and experimental determination of the material intrinsic length scale of strain gradient plasticity theory from micro- and nano-indentation experiments. International Journal of Plasticity 20 (6), 1139–1182.

Abu-Lebdeh, T.M., Voyiadjis, G.Z., 1993. Plasticity-Damage Model for concrete under cyclic multiaxial loading. Journal of Engineering Mechanics 119, 1993.

Ananiev, S., Ozbolt, J., 2004. Plastic-damage model for concrete in principal directions. In: Li, V., Leung, C.K.Y., William, K.J., Billington, S.L. (Eds.), Fracture Mechanics of Concrete Structures, FraMCoS-5, Vail, Colorado, USA, pp. 271–278.

Bazant, Z.P., 1978. On endochronic inelasticity and incremental plasticity. International Journal of Solids Structures 14, 691–714.

Bazant, Z.P., Kim, S-S., 1979. Plastic-fracturing theory for concrete. Journal of the Engineering Mechanical Division (ASCE) 105, 407–428.

Brünig, M., Ricci, S., 2005. Nonlocal continuum theory of anisotropically damaged metals. International Journal of Plasticity 21 (7), 1346–1382.

Carol, I., Rizzi, E., William, K.J., 2001. On the formulation of anisotropic elastic degradation. II. Generalized pseudo-Rankine model for tensile damage. International Journal of Solids and Structures 38, 519–546.

Chen, E.S., Buyukozturk, O., 1985. Constitutive model for concrete in cyclic compression. Journal of the Engineering Mechanics Division, ASCE 111, 797–814.

Chen, A.C.T., Chen, W.F., 1975. Constitutive relations for concrete. Journal of the Engineering Mechanical Division, ASCE 101, 465–481.

Chow, C.L., Wang, J., 1987. An anisotropic theory of elasticity for continuum damage mechanics. International Journal of Fracture 33, 2–16.

Coleman, B.D., Gurtin, M.E., 1967. Thermodynamics with internal state variables. Journal Chemical Physics 47 (2), 597–613.

Cordebois, J.P., Sidoroff, F., 1979. Anisotropic damage in elasticity and plasticity. Journal de Mecanique Theorique et Applilquee (Numero Special), 45–60.

Dragon, A., Mroz, Z., 1979. A continuum model for plastic-brittle behavior of rock and concrete. International Journal of Engineering Science 17, 121–137.

Este, G., Willam, K.J., 1994. A fracture-energy based constitutive formulation for inelastic behavior of plain concrete. Journal of Engineering Mechanics, ASCE 120, 1983–2011.

Gatuingt, F., Pijaudier-Cabot, G., 2002. Coupled damage and plasticity modeling in transient dynamic analysis of concrete. International Journal of Numerical and Analytical Methods in Geomechanics 26, 1–24.

Grassl, P., Lundgren, K., Gylltoft, K., 2002. Concrete in compression: a plasticity theory with a novel hardening law. International Journal of Solids and Structures 39, 5205–5223.

Hansen, E., William, K., Carol, I., 2001. A two-surface anisotropic damage/plasticity model for plain concrete. In: de Borst, R., Mazars, J., Pijaudier-Cabot, G., van Mier, J.G.M. (Eds.), Fracture Mechanics of Concrete Structures. Balkema, Lisse, pp. 549–556.

Imran, I., Pantazopoulu, S.J., 2001. Plasticity model for concrete under triaxial compression. Journal of Engineering Mechanics 127, 281–290.

Jason, L., Pijaudier-Cabot, G., Huerta, A., Crouch, R., Ghavamian, S., 2004. An elastic plastic damage formulation for the behavior of concrete. In: Li, V., Leung, C.K.Y., William, K.J., Billington, S.L. (Eds.), Fracture Mechanics of Concrete Structures, Ia-FraMCos-5, Vail, Colorado, USA, pp. 549–556.

Kachonov, L.M., 1958. On the creep fracture time. Izvestiya Akademii Nauk USSR Otd. Tech. 8, 26–31 (in Russian).

Karabinis, A.I., Kiousis, P.D., 1994. Effects of confinement on concrete columns: a plasticity theory approach. ASCE Journal of Structural Engineering 120, 2747–2767.

Karsan, I.D., Jirsa, J.O., 1969. Behavior of concrete under compressive loadings. Journal of the Structural Division, ASCE 95, 2535–2563.

Krajcinovic, D., 1983. Continuum damage mechanics. Applied Mechanics Reviews 37, 1–6.

Krajcinovic, D., 1985. Continuous damage mechanics revisited: basic concepts and definitions. Journal of Applied Mechanics 52, 829–834.

Krajcinovic, D., 1996. Damage mechanics. In: North-Holland Series in applied mathematics and mechanics, vol. 41. North-Holland, Amsterdam, 761p.

Kratzig, W., Polling, R., 2004. An elasto-plastic damage model for reinforced concrete with minimum number of material parameters. Computers and Structures 82, 1201–1215.

Kupfer, H., Hilsdorf, H.K., Rusch, H., 1969. Behavior of concrete under biaxial stresses. ACI Journal 66, 656–666.

Lee, J., Fenves, G.L., 1998. A plastic-damage model for cyclic loading of concrete structures. Journal of Engineering Mechanics, ASCE 124, 892–900.

Loland, K.E., 1980. Continuous damage model for load-response estimation of concrete. Cement & Concrete Research 10, 395–402.

Lubarda, V.A., Kracjinvovic, D., Mastilovic, S., 1994. Damage model for brittle elastic solids with unequal tensile and compressive strength. Engineering Fracture Mechanics 49, 681–697.

Lubliner, J., Oliver, J., Oller, S., Onate, E., 1989. A plastic-damage model for concrete. International Journal of Solids Structures 25, 299–326.

Mazars, J., Pijaudier-Cabot, G., 1989. Continuum damage theory- Application to concrete. Journal of Engineering Mechanics 115, 345–365.

Menetrey, Ph., Willam, K.J., 1995. Triaxial failure criterion for concrete and its generalization. ACI Structural Journal 92, 311–318.

Menzel, A., Ekh, M., Runesson, K., Steinmann, P., 2005. A framework for multiplicative elastoplasticity with kinematic hardening coupled to anisotropic damage. International Journal of Plasticity 21 (3), 397–434.

Murakami, S., Ohno, N., 1981. A continuum theory of creep and creep damage. Proceedings of the Third IUTAM Symposium on Creep in Structures. Springer, Berlin, pp. 422–444.

Onate, E., Oller, S., Oliver, S., Lubliner, J., 1988. A constitutive model of concrete based on the incremental theory of plasticity. Engineering Computations 5, 309–319.

Ortiz, M., 1985. A constitutive theory for the inelastic behavior of concrete. Mechanics of Materials 4 (1), 67–93.

Ortiz, M., Popov, E.P., 1982. Plain concrete as a composite material. Mechanics of Material 1, 139–150.

Resende, L., Martin, J.B., 1984. A progressive damage continuum model for granular materials. Computer Methods in Applied Mechanics and Engineering 42, 1–18.

Schreyer, H.L., 1983. Third-invariant plasticity theory for frictional materials. Journal of Structural Mechanics 11, 177–196.

Simo, J.C., Honein, T., 1990. Variational formulation, discrete conservation laws, and path domain independent integrals for elasto-viscoplasticity. Journal of Applied Mechanics, Transactions of ASME 57, 488–497.

Simo, J.C., Hughes, T.J.R., 1998. Computational inelasticity. Interdisciplanary Applied Mathematics. Springer, New York.

Simo, J.C., Ju, J.W., 1987a. Strain and stress-based continuum damage. Model. Part I: formulation. International Journal of Solids and Structures 23, 821–840.

Simo, J.C., Ju, J.W., 1987b. Strain- and stress-based continuum damage models. Part II: computational aspects. International Journal for Solids and Structures 23, 841–869.

Voyiadjis, G.Z., Abu-Lebdeh, T.M., 1994. Plasticity model for concrete using the bounding surface concept. International Journal of Plasticity 10, 1–21.

Voyiadjis, G.Z., Kattan, P.I., 1992a. A plasticity-damage theory for large deformations of solids. Part I: Theoretical formulation. International Journal of Engineering Science 30, 1089–1108.

Voyiadjis, G.Z., Kattan, P.I., 1992b. Finite strain plasticity and damage in constitutive modeling of metals with spin tensors. Applied Mechanics Reviews 45, 95–109.

Voyiadjis, G.Z., Kattan, P.I., 1999. Advances in Damage Mechanics: Metals and Metals Matrix Composites. Elsevier, Oxford.

Voyiadjis, G.Z., Park, T., 1997. Anisotropic damage effect tensors for the symmetrization of the effective stress tensor. Journal of Applied Mechanics, ASME 64, 106–110.

Voyiadjis, G.Z., Abu Al-Rub, R.K., Palazotto, A.N., 2003. Non-local coupling of viscoplasticity and anisotropic viscodamage for impact problems using the gradient theory. Archives of Mechanics 55 (1), 39–89.

Voyiadjis, Z.V., Abu Al-Rub, K.R., Palazotto, A.N., 2004. Thermodynamic framework for coupling of non-local viscoplasticity and non-local anisotropic viscodamage for dynamic localization problems using gradient theory. International Journal of Plasticity 20, 981–1038.

William, K.J., Warnke, E.P., 1975. Constitutive model for the triaxial behavior of concrete. International Association of Bridge and Structural Engineers, Seminar on Concrete Structure Subjected to Triaxial Stresses, Paper III-1, Bergamo, Italy, May 1974, IABSE Proceedings 19.

Wu, J.U., Li, J., Faria, R., 2006. An energy release rate-based plastic-damage model for concrete. International Journal of Solids and Structures 43, 583–612.

Yazdani, S., Schreyer, H.L., 1990. Combined plasticity and damage mechanics model for plain concrete. Journal of the Engineering Mechanics Division, ASCE 116, 1435–1450.